European Polymer Journal 177 (2022) 111438

Contents lists available at ScienceDirect

European Polymer Journal

journal homepage: www.elsevier.com/locate/europolj

Crosslinked bacterial cellulose hydrogels for biomedical applications

Ana P.C. Almeida [a], João N. Saraiva [a], Gonçalo Cavaco [b], Raquel P. Portela [b], Catarina R. Leal [a,c], Rita G. Sobral [b], Pedro L. Almeida [a,c,*]

[a] I3N-CENIMAT, Materials Science Department, School of Science and Technology, NOVA University Lisbon, 2829-516 Caparica, Portugal
[b] Associate Laboratory i4HB – Institute for Health and Bioeconomy, NOVA School of Science and Technology, NOVA University Lisbon, Caparica, Portugal and UCIBIO-Applied Biomolecular Sciences Unit, School of Science and Technology, NOVA University Lisbon, 2829-516 Caparica, Portugal
[c] Physics Department, Instituto Superior de Engenharia de Lisboa, Instituto Politécnico de Lisboa, 1959-007 Lisbon, Portugal

ARTICLE INFO

Keywords:
Biomaterials
Biomedical applications
Bacterial cellulose
Crosslinking
Wound dressings

ABSTRACT

Recently, increasing attention has been given to bacterial cellulose-based membranes to be applied as dressings for healing purposes. Bacterial cellulose (BC) is an attractive biomaterial due to its unique structural characteristics such as high porosity, high water retention capacity, high mechanical strength, low density, and biodegradability. One drawback of bacterial cellulose hydrogels is that, after the first dehydration, the water retention capacity is hindered. In this work we produced, modified, and characterized hydrated and de-hydrated BC membranes for biomedical applications. Two crosslinking methods were adopted (using citric acid and epichlorohydrin as crosslinking agents), and the results obtained from the characterization, such as water retention capacity, mechanical properties or contact angle, were compared to those of unmodified bacterial cellulose. We demonstrate that the cross-linked bacterial cellulose membranes present physical properties suitable to be used as wound dressings when hydrated, or as exuding wound dressings, when dehydrated.

1. Introduction

Cellulose is the most abundant natural polymer in the world and of great economic importance being a linear homopolysaccharide composed by *D-glucopyranose* units linked by glycosidic bonds [1]. The largest source of this material is the cell wall of plants, but it is also produced by fungi, protozoa and prokaryotes [2]. Much of the cellulose by-products, such as paper and textiles are extracted from cotton and wood. But issues of sustainability and preservation of the environment have led to the search for alternative non-conventional materials, such as bacterial cellulose (BC). For many industrial applications, vegetable cellulose is inconvenient, due to its association with other biopolymers such as hemicellulose and lignin [3]. BC is also an attractive biomaterial due to its unique structural characteristics such as high porosity, high water retention capacity, high mechanical strength even in the hydrated state, low density, and biodegradability by many microorganisms, although, not by the human body [4]. Another advantage of bacterial cellulose is the possibility of synthesis in a short time, independent of long and extensive agroforestry crops, by different genera of microorganisms. The genus *Komagataeibacter* is the most studied, from which the species *K. rhaeticus* stands out for its high production capacity from different carbon sources (glucose, fructose, molasses, glycerol, or other organic substrates) and nitrogen [5], which is an important advantage of this microorganism in industrial application [6]. Under static cultivation conditions, a BC-biofilm of tuneable thickness is formed to maintain high oxygenation of the cells near the surface, and to serve as a protective barrier against drying and radiation. Chemically the BC structure is identical to vegetal cellulose, being composed by *β-1-4*-linked glucosidic chains. These chains are organized into moderately crystalline BC fibres containing hydroxyl groups on their surfaces. These BC fibres are composed by microfibril units with diameters of around 3 nm, having themselves diameters of about 30 nm [3]. These randomly oriented fibres form a non-woven, highly hydrated gel during the aqueous fermentation conditions. This fact provides BC with superior properties compared to vegetable cellulose. Ribbon-shaped microfibres provide bacterial cellulose with peculiar mechanical properties, such as high tensile strength, elasticity, durability, and high-water retention capacity [7]. This biopolymer can absorb over 200 times its own mass in water. BC is biocompatible, inert, non-toxic, and non-allergenic and thus its use as dressings results in better healing. It provides a moist environment for

Abbreviations: BC, Bacterial Cellulose; CA, Citric Acid; ECH, Epichlorohydrin.

* Corresponding author at: Physics Department, Instituto Superior de Engenharia de Lisboa, Instituto Politécnico de Lisboa, 1959-007 Lisbon, Portugal.
E-mail address: pedro.almeida@isel.pt (P.L. Almeida).

https://doi.org/10.1016/j.eurpolymj.2022.111438
Received 12 June 2022; Received in revised form 19 July 2022; Accepted 20 July 2022
Available online 25 July 2022

wounds, presenting adequate structure and mechanical robustness. It is also promising for the incorporation of antimicrobial agents and can be used in several fields of health sciences, in applications such as structures for bone regeneration, drug delivery systems, new vascular grafts, or supports for tissue engineering [8]. BC has already been used quite successfully in wound-healing applications, proving that it could become a high-value product in the field of biotechnology [9]. Wound dressing cellulose hydrogels should ideally display high porosity, with a nanopore structure and should keep the wound moist during the healing process [10].

Hydrated dressings of BC have proven healing potential, however, due to the water content, the accumulation of secretion in exudative injuries may occur. For these exuding wounds, as well as for diapers dressing and sanitary pads, dehydrated BC membranes might be used. Unmodified BC have a high-water retaining capacity (>200x its own weight) and a low water release [11]. However, upon dehydration, the structure of BC collapses due to the evaporation of water, reducing its ability to re-swell. To revert this drawback, one possible solution is the crosslinking of the BC prior to the first dehydration of the membranes [12]. Several other modifications have been proposed to counteract the disadvantageous consequences of the first BC dehydration, as for example, the production of BC-fibrin or BC-gelatine composites, resulting in improvement of their physical properties [13,14]. Considering that the water retention capacity of the bacterial cellulose is reduced after the first dehydration, meaning that after drying for the first time the BC will not be able to absorb the same amount of water with respect to its own weight, two methods of BC crosslinking were used to counteract this fact. By crosslinking the BC, a 3D structure is promoted that reduces the collapse of the pore structure, and thus sustains a higher value of water retention capacity of the BC membranes. BC crosslinking is typically obtained by linking at least two hydroxyl groups of single cellulose molecules or two or more hydroxyl groups of adjacent cellulose molecules, resulting in a stiffer polymer and preserving its 3D structure [15].

In this work, chemical modifications were performed on bacterial cellulose, by crosslinking the biopolymer with two different crosslinkers, namely Citric Acid (CA) and Epichlorohydrin (ECH), to increase its water retention capacity after the first dehydration. CA is a tricarboxylic acid based on propane-1,2,3-tricarboxylic acid with a hydroxy substituent at position 2. Citric acid is a very suitable crosslinker for wound dressing, not only due to its non-toxicity, but also due to the stable crosslinking bonds that it forms with cellulose. Moreover, CA is widely accessible and very low cost, which makes it a very interesting reagent for industrial applications [16]. ECH is an epoxide compound, based on 1,2-epoxypropene in which one of the methyl hydrogens is substituted by chlorine. It has moderate toxicity and has been described that short-term inhalation of this compound might cause irritation to the eyes, respiratory tract and skin and might be a human carcinogen. However, if ECH fully reacts with BC, it becomes inoffensive [17]. There are several works in literature that demonstrated the biocompatibility of ECH crosslinked polymers. For instance, Yang et al. [18] after conducting cytotoxicity assays, stated that polyglycerol hydrogel crosslinked with epichlorohydrin could be used safely in biomedical applications.

These modified membranes were characterized, and their properties were compared with unmodified BC.

2. Materials and methods

2.1. Bacterial cellulose production

The *Komagateibacter rhaeticus* strain DSM-16663 was obtained from the German Collection of Microorganisms and Cell Cultures GmbH (DSMZ) and reconstituted accordingly to the DSMZ instructions. The strain was grown in DSMZ medium 1044 (glucose 50.0 g/L, yeast extract 5.0 g/L and agar 15.0 g/L, pH 6.5). The plates were incubated at 28 °C for 2–3 days.

To produce BC, single colonies were used to inoculate the growth media) yeast extract 4.0 g/L, anhydrous disodium phosphate 2.0 g/L, heptahydrate magnesium sulphate 0.8 g/L and ethanol 20 g/L [19]. The cultures were grown statically at 28 °C until the BC pellicles reached the desired thickness, for approximately 10–15 days.

After the 10–15 days of incubation, the BC discs were removed from the culture, washed twice with distilled autoclaved water to ensure the complete removal from the BC matrix of bacterial cells, cell debris, and remaining compounds of the culture. After this first step, the membranes were washed in absolute ethanol for two hours with gentle agitation and again twice in hot distilled autoclaved water. The final step consisted in immersing the BC disks statically in 0.1 M NaOH solution, for 48 h. After this alkaline treatment, the BC disks were again washed twice with autoclaved water until a neutral pH of 7 was achieved. After the washing procedure, the BC disks were stored in the hydrated form (in Milli-Q water) at 4 °C, having thicknesses of around 1–2 mm.

2.2. Bacterial cellulose crosslinking

Two methods of crosslinking were applied, one using Citric Acid and the other Epichlorohydrin. Although we tested higher percentages, we hereby describe the physical properties of the crosslinked BC for the range of percentages, specific for each crosslinker, that clearly demonstrate their influence in the properties of BC. The other crosslinker percentages tested did not present improved results and for this reason were not included. Based on this variation, one amount of each crosslinker was chosen as the most suitable amount of crosslinker for this application and was used throughout the work. The schematic representation of the BC crosslinking with both crosslinkers can be seen in Fig. 1.

2.3. Citric acid crosslinking

To perform the BC crosslinking with CA, a mixture of sodium dihydrogen phosphate (H_2NaO_4P) and sodium hydrogen carbonate ($NaHCO_3$) (1:1 mass ratio) was used as catalyst. Aqueous solutions containing different amounts of CA (10 %, 20 %, 30 % and 50 % weight percentage with respect to the hydrated BC membrane), and catalyst (50 % weight percentage with respect to CA) were prepared by magnetic stirring at room temperature. The unmodified BC membranes were added to these aqueous solutions and incubated under magnetic stirring at 40 °C for 24 h. The BC membranes were then crosslinked under reflux at 150 °C for 75 min. Subsequently, the membranes were washed at least 3 times, for 30 min each, with Milli-Q water to remove the residual H_2NaO_4P and $NaHCO_3$, and the unreacted CA. The membranes were then kept at 4 °C until further use. The crosslinking reaction between the hydroxyl groups of BC and citric acid is shown in Fig. 1 A.

2.4. Epichlorohydrin crosslinking

To perform the BC crosslinking with ECH, aqueous solutions containing different amounts of ECH (0.5 %, 1 %, 2 %, 5 % and 10 % weight percentage with respect to the hydrated BC membrane) were prepared by magnetic stirring at room temperature. The unmodified BC membranes were added to the aqueous solutions and were crosslinked under reflux at 60 °C for 120 min. The pH value of the aqueous solutions was adjusted to 9 with a 0.1 M solution of NaOH. Subsequently, the membranes were washed at least 3 times, for 30 min each, with Milli-Q water to remove the residual NaOH and unreacted ECH. The membranes were then kept at 4 °C until further use. The crosslinking reaction between the hydroxyl groups of the bacterial cellulose and Epichlorohydrin is shown in Fig. 1B.

2.5. Water loss rate

The water loss assays were conducted by placing BC samples in a

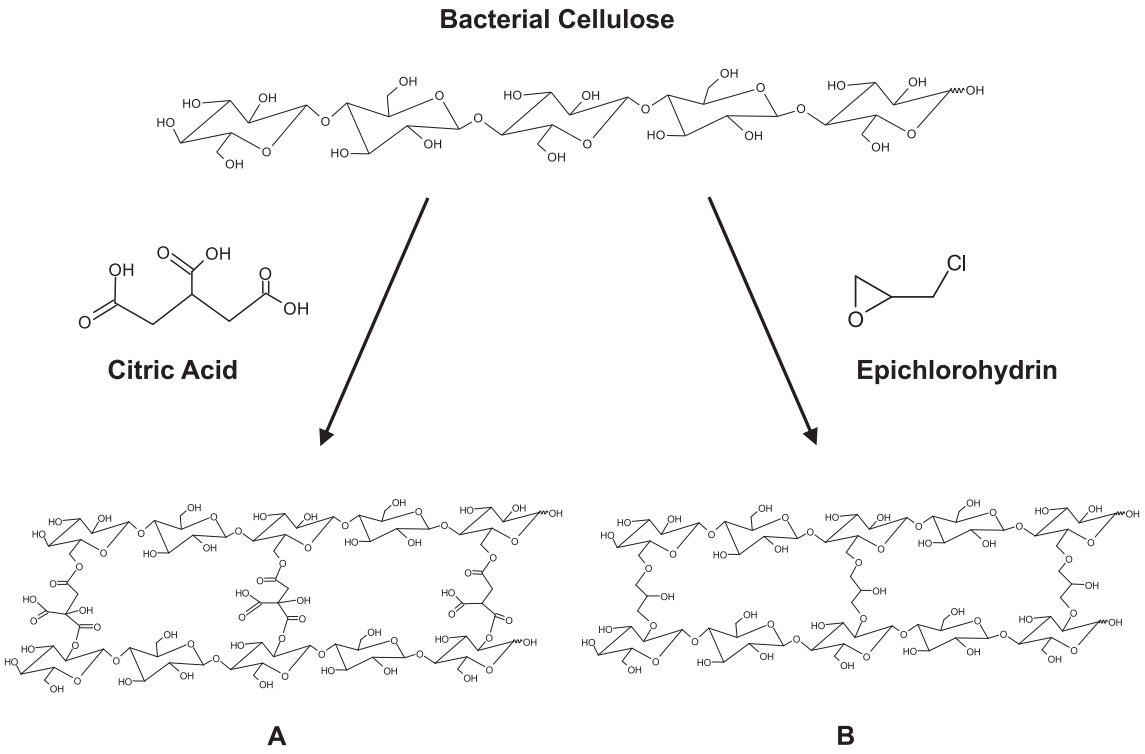

Fig. 1. Schematic crosslinking mechanism between the hydroxyl groups of the bacterial cellulose (**A**) Citric Acid and (**B**) Epichlorohydrin.

ventilated oven at 35 °C and by weighting them at periodic time intervals until a constant weight is reached.

2.6. Water uptake rate and water retention capacity

The hydrophilic properties of BC membranes were studied through the water absorption capacity as a function of time. The water absorption capacity depends on the degree of interaction between water and the cellulose molecules. Furthermore, the water absorption capacity is related to the structure of the BC membrane, since the larger is the size of the pores in the membrane, the greater is the water absorption capacity and, consequently, the greater is the degree of water retention.

To test the water retention capacity (maximum water absorption) of the different membranes, crosslinked with different amounts of each crosslinker, the membranes were initially weighted after dehydration and 48 h after being placed in Milli-Q water, *i.e.*, after full hydration.

To estimate the water retention capacity the following expression was used, $H_2O\% = \frac{m_h - m_d}{m_h} H_2O\% = \frac{m_h - m_d}{m_h}$, in which m_h is the hydrated mass of the membrane (BC + H_2O), and m_d is the dehydrated mass of the membrane (only BC).

To measure the water uptake rate, disks with a diameter of approximately 50 mm were used. After dehydration, they were initially weighted and placed in Milli-Q water and left at room temperature. At different pre-established times, the discs were removed using tweezers, carefully placed on absorbent paper, to remove the water excess at the surface and then weighted.

2.7. FTIR-ATR characterization

To characterize the chemical structure of the produced membranes, Fourier transform infrared spectroscopy – attenuated total reflectance (FTIR–ATR) analysis was performed. The identification of specific functional groups reveals chemical changes that occurred in the unmodified structure. The FTIR–ATR spectroscopy characterization of the BC membranes was conducted using an attenuated total reflectance (ATR) sampling accessory (Smart iTR) equipped with a single bounce diamond crystal on a Thermo Nicolet 6700 Spectrometer. The spectra were acquired with a 45° incident angle in the range of 4500–540 cm^{-1} and with a 4 cm^{-1} resolution.

2.8. Mechanical properties of the dehydrated membranes

The mechanical tensile tests were carried out using a static-dynamic miniature testing machine *inspect micro LC 100 N* from *Hegewald & Peschke Meβ-und Prüftechnik GmbH* with a 100 *N* load cell. Rectangular pieces of the BC membranes with dimensions 0.5 × 3.0 cm^2 were cut radially from the membrane disks. At least 3 tests were conducted for each membrane. The rectangular samples were tested uniaxially in tension with a strain rate of 0.5 $mm.min^{-1}$ along their widest dimension, at room temperature. The initial gauge length l_0 for each sample was 10 mm, the width of the test samples was 5 mm and the thickness of the membranes used for the tensile tests were in the range of 50–100 μm when dehydrated. From these tensile tests, mechanical properties such as the ultimate tensile strength (UTS), strain at break and the *Young*'s modulus (elastic modulus), were determined.

2.9. Mechanical properties of the hydrated membranes

The rheological characterization of BC membranes was performed with a Modular Compact Rheometer MCR 502 (*Anton Paar*, Madrid, Spain), using a parallel-plate geometry with a sandblasted surface, with a diameter of 25 mm. Oscillatory shear measurements were performed to evaluate the storage G' and the loss G" moduli within the linear viscoelastic regime (LVR) in which the moduli are strain independent. Measurements were carried out under a constant strain of 0.1 % in the angular frequency range of 0.6 to 100 rad/s, at two different temperatures, 25 °C and 37 °C.

The BC membranes were produced in containers with similar diameter (25 mm) as the one of the rheometer geometry to assure a correct fit and avoid sample cut. Sample thicknesses were obtained in the range of 1.5 ± 0.7 mm. Before loading the BC samples in the rheometer plate, the membrane water excess was removed by a brief

both side deposition on filter paper.

2.10. Contact angle measurements

To determine the water contact angles formed on the surface of BC membranes, measurements were performed using an OCA20 contact angle measuring instrument (*DataPhysics Instruments GmbH, Filderstadt, Germany*). Probe liquid micro drops (volume ≈ 5 μL of Milli-Q water) were generated with an electronic micrometric syringe and deposited on the sample surface. The contact angle was determined at the moment of drop deposition and settlement (t = 0 s) and its evolution was followed for 120 s with a system video camera and recorded at rate of 2 frames per second. The contact angle was determined by fitting the shape of the drop (in the captured video image) to the Young-Laplace equation, which relates the interfacial tension to the shape of the drop. A total of six drops of the probe liquid were dispensed and each drop was placed in a different region of the membrane. All measurements were performed at room temperature, using dry membranes of 1.0 × 2.0 cm^2. The results correspond to the average of six independent measurements. The probe liquid used was ultrapure water. Image acquisition, analysis and contact angle determination were performed using the *SCA20 v.4.3.12* and *v.4.3.16* software (*DataPhysics Instruments GmbH, Filderstadt, Germany*).

2.11. SEM analysis

Scanning Electron Microscopy (SEM) images of the surface morphology of the membranes were obtained using a SEM DSM962 model from Zeiss. Gold was deposited on the samples by sputtering in an *Ar* atmosphere, using a 20 mA current, for 30 s at a deposition rate of 3 $Å.s^{-1}$. Images were obtained for an acceleration voltage of 5 kV.

3. Results and discussion

Bacterial cellulose membranes produced by the species *K. rhaeticus* were crosslinked with two different compounds (Citric Acid (CA) and Epichlorohydrin (ECH)) using different percentages, to determine the crosslinking procedure that results in the best physical properties of the membranes for biomedical applications.

3.1. Water retention capacity

In Table 1 and Table 2, the maximum water retention capacity of the several studied samples, unmodified and crosslinked with different percentages of both crosslinkers ECH and CA, are presented.

This work from hereon was focused on two type of bacterial cellulose samples: BC crosslinked with 2 % ECH and BC crosslinked with 50 % CA, which properties were interpreted, comparing them with the ones of unmodified BC. These two samples (BC crosslinked with 2 % ECH and BC crosslinked with 50 % CA) are the ones for each crosslinking method, that present the lowest reduction in the water retention capacity, when compared with the unmodified BC (prior to the first de-hydration). The sample crosslinked with 2 % ECH underwent a water retention capacity reduction of 22.3 % while the sample crosslinked with 50 % CA underwent a water retention capacity reduction of 12.7 %. Being so, the sample that showed the highest water retention capacity, proceeding from the dehydrated state, was the sample crosslinked with 50 % CA which can be due to the presence of a higher number of hydroxyl groups after crosslinking on the surface of the BC fibres when compared to the sample crosslinked with ECH [20].

Table 1
Water retention capacity (in weight percentage) of samples crosslinked with ECH as a function of the amount of crosslinking agent.

	Unmodified BC	0.5 %	1.0 %	2.0 %	5.0 %	10.0 %
Before the 1st dehydration	98.5 ± 0.2	99.3 ± 0.2	99.4 ± 0.3	99.3 ± 0.2	99.2 ± 0.4	98.9 ± 0.5
After the 1st dehydration	69.9 ± 0.7	73.6 ± 0.8	74.9 ± 0.2	77.0 ± 0.2	69.9 ± 0.4	63.6 ± 0.7

Table 2
Water retention capacity (in weight percentage) of samples crosslinked with CA as a function of the amount of crosslinking agent.

	Unmodified BC	10.0 %	20.0 %	30.0 %	50.0 %
Before the 1st dehydration	98.5 ± 0.2	97.1 ± 0.7	97.2 ± 0.5	93.8 ± 0.3	95.0 ± 0.6
After the 1st dehydration	69.9 ± 0.7	75.1 ± 0.2	75.2 ± 0.6	75.9 ± 0.7	82.3 ± 0.4

3.2. Water uptake rate

The samples were weighted from t = 0 until t = 1440 min and the results obtained for three different samples were plotted in Fig. 2.

The water uptake capacity for unmodified BC, BC crosslinked with 50 % CA and crosslinked with 2 % ECH is presented in Fig. 2. The data was calculated by dividing the time dependent mass values of BC + H_2O by their respective final mass value (fully hydration) for normalization. The water uptake kinetics showed that the water uptake rate was approximately linear during the first 120 min for all studied samples, approximately 0.002 g/min (per final weight of 1 g of BC + H_2O) for the unmodified sample, approximately 0.003 g/min (per final weight of 1 g of BC + H_2O) for the sample crosslinked with 2 % ECH and approximately 0.006 g/min (per final weight of 1 g of BC + H_2O) for the sample crosslinked with 50 % CA. The differences observed in the water uptake capacity between the different samples could be explained by their respective porous structure, since the water molecules are thought to be physically trapped by the delicate network structure of the membranes. The BC membranes consists of randomly arranged fibrils having a large quantity of empty spaces between them [21,22]. The crosslinking of the BC membranes is responsible for maintaining the porous structure that BC possesses before the first dehydration. Being so, the crosslinked membranes present higher water uptake rates than the unmodified BC, since by capillarity the water fills those voids more efficiently than on a collapsed structure such as the one on unmodified BC.

3.3. Water loss rate

Average values of the mass obtained for the samples tested at each time point were plotted in Fig. 3 A. The data presented was calculated by dividing the time dependent values of BC + H_2O mass by its initial value for normalization. There was no measurable difference in the water loss rate between samples from unmodified BC and crosslinked BC (with AC and ECH). This is in accordance with the fact that the assay started with the BC membranes fully hydrated (Fig. 3 B), with the pores strained to their maximum dimensions, so that the access of the water molecules to the atmosphere was approximately the same for all samples [23]. Close to the dried state (Fig. 3 C), the water loss rate was expected to be different from sample to sample and slightly higher in the crosslinked samples due to their structure, but the weight values obtained at this stage of the assays were so small (≈ 0.5 mg), that eventual differences were not observable.

BC can hold an enormous amount of water without losing its structural coherence due to the large number of hydrogen bonding interactions existing between water and the hydroxyl groups present in the BC fibres [24]. During the first 300 min, a water loss rate of approximately 0.003 g/min per initial weight of 1 g of BC + H_2O, was observed. After 300 min, the water loss rate was dramatically reduced, and a constant mass value (BC without water) was obtained only after 24 h of the beginning of the assay. Similar results were obtained for unmodified

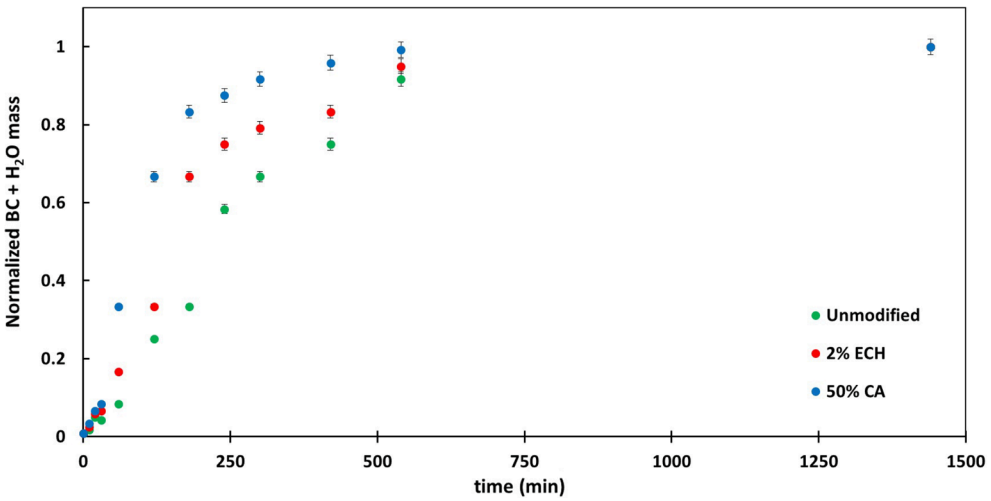

Fig. 2. Water uptake assays of BC membranes (unmodified BC; crosslinked with 50 % CA and crosslinked with 2 % ECH), normalized BC + H_2O mass (normalized by its maximum value).

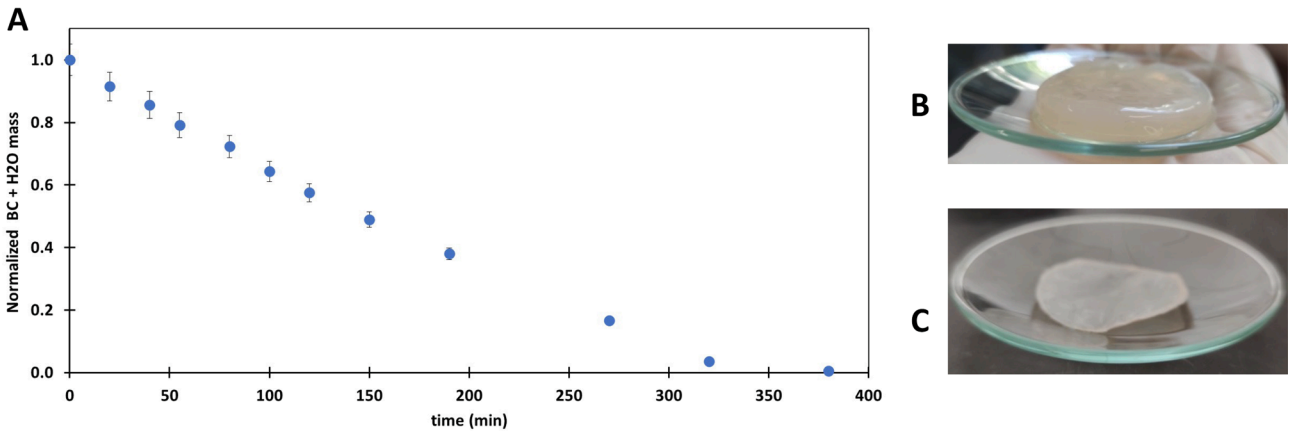

Fig. 3. Water loss assay of a BC membrane. (**A**) normalized BC + H_2O mass (normalized by its initial value) over time (**B**) fully hydrated membrane (**C**) fully dehydrated membrane.

BC [25].

3.4. FTIR-ATR characterization

FTIR spectroscopy was used to identify the functional groups of the modified and unmodified BC membranes produced. In the IR spectra

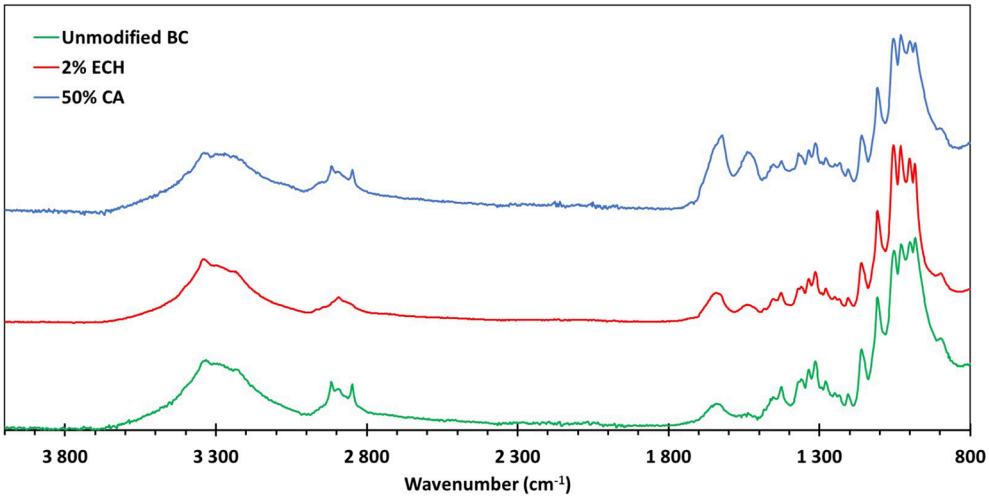

Fig. 4. Fourier-transformed infrared spectra of bacterial cellulose membranes before and after crosslinking with 2 % ECH and 50 % CA.

obtained for the prepared membranes (Fig. 4) the characteristic peaks of cellulose were observed.

A broad absorption peak of –OH stretching vibration at 3332 cm^{-1}, due to the intermolecular hydrogen bonds [25], was observed for the three membranes. The peak around 2890 cm^{-1}, that corresponds to the aliphatic –CH stretching vibration characteristic of carbohydrates was also present in all the samples, being less intense in the ECH crosslinked sample. In the three spectra, the several peaks in the region between 1000 and 1200 cm^{-1} are characteristic of C=O groups of the primary hydroxyl strong stretching vibration, that may be attributed to the cellulose structure [26]. The peak at 1641 cm^{-1} corresponds to the $–CH_2$ bending vibration, being more intense in the CA crosslinked sample. The peaks associated to C–OH stretching and C–O–C bending vibrations that occur at 1031 cm^{-1} and 1107 cm^{-1} were also observed for all the membranes produced [27]. The spectral signatures of BC and of the modified BC with 2 % ECH form were highly overlapped [28]. The peak at 1735 cm^{-1}, typical of ester carbonyl groups, was expected to be present in the BC modified by citric acid [12,26], but was not observed.

3.5. Mechanical properties of the dehydrated membranes

The mechanical properties of bacterial cellulose depend on the producing strain, as well as on the fermentation conditions. For instance, the degree of crystallinity of BC, strongly influences its mechanical properties [29].

The BC mechanical properties have already been determined for single isolated fibres, evidencing the extraordinary specific tensile strength (normalized by specific density). The specific tensile strength of the BC fibres can achieve 598 $MPa.g^{-1}.cm^3$, which is considerably higher than the novel lightweight steel (227 $MPa.g^{-1}.cm^3$) [30].

In this work, the mechanical properties were determined not for isolated fibres but for the dehydrated membranes, using uniaxial tensile testing. In Fig. 5, plots of the typical stress-strain behaviour obtained for each membrane are shown. The differences in the mechanical behaviour between the three studied membranes were obvious. The more pronounced differences were the higher tensile strength of the crosslinked samples and consequently their lower plastic deformation.

In Table 3, the average values of the mechanical properties obtained for the different BC membranes are displayed and were extracted from the tensile tests.

In Fig. 5, the crosslinking of the BC membranes induced a stiffer and more fragile behaviour, when compared with the unmodified membrane. The unmodified BC samples attained a high value of strain at break (39 %), while for the crosslinked samples, this value decreased to 7.2 % or 3.6 % for the crosslinking with 2 % ECH and 50 % CA, respectively. This stiffer and more fragile behaviour was not only evident in the strain but also in the ultimate tensile strength (UTS) and the *Young*'s modulus. The unmodified BC samples presented an UTS of 33.9 MPa and a *Young*'s modulus of 1.62 GPa, while the samples crosslinked with 2% ECH presented an UTS of 162.2 MPa and a *Young*'s modulus of 2.77 GPa and the sample crosslinked with 50% CA presented an UTS of 72.7 MPa and a *Young*'s modulus of 2.89 GPa. Similar mechanical properties have been described for the unmodified BC membranes [31–34]. These obvious differences in behaviour are expected in general, when comparing a non-crosslinked polymer with the same polymer after crosslinking. The crosslinking of the BC membranes hinders or prevents the movement of the BC molecules (chains' mobility) that is necessary for the existence of plastic deformation. In fact, the unmodified BC membranes presented a high plastic deformation while the crosslinked samples displayed an almost exclusive elastic behaviour, with a higher elastic modulus, almost twice as higher as the one obtained for the unmodified BC.

Table 3
Mechanical properties of the dehydrated BC membranes.

	Young's modulus (GPa)	Ultimate tensile strength (MPa)	Strain at break (%)
Unmodified BC	1.62 ± 0.01	33.9 ± 0.2	39 ± 16
2% ECH	2.77 ± 0.02	162.2 ± 0.6	7.2 ± 0.8
50% CA	2.89 ± 0.02	72.7 ± 0.3	3.6 ± 0.2

As can be perceived from the data in Table 3, the UTS is slightly over 2-fold higher in the case of the ECH crosslinked sample when compared with the CA crosslinked sample. One explanatory hypothesis for this difference is that ECH may be a more efficient crosslinker in these cellulosic systems. An alternative hypothesis is that the ECH crosslinking molecular bonds may require more energy to be broken than the CA bonds. Finally, a third hypothesis is that the crosslinking reaction temperature (150 °C for CA and 60 °C for ECH), may influence the mechanical strength of the BC fibres.

In the dehydrated state, the unmodified BC sample was much more ductile than the crosslinked ones, which were more brittle, although for the proposed application (wound dressings) all samples presented suitable properties, being mechanically robust and resilient, with mechanical properties compatible with those of the human skin [35].

3.6. Mechanical properties of the hydrated membranes

The viscoelastic properties of BC membranes can be observed in

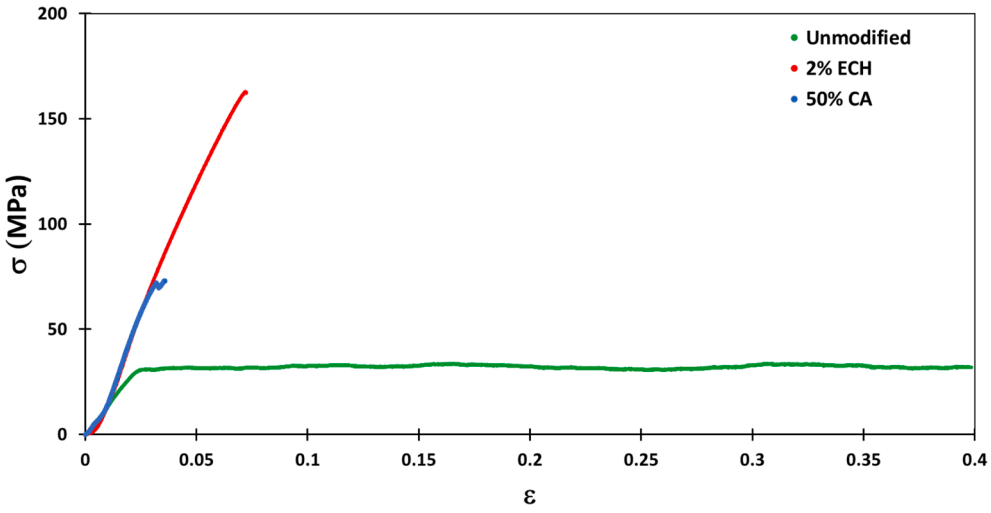

Fig. 5. Stress-strain curves obtained in the tensile tests for BC membranes: unmodified BC; crosslinked with 50 % CA and crosslinked with 2 % ECH.

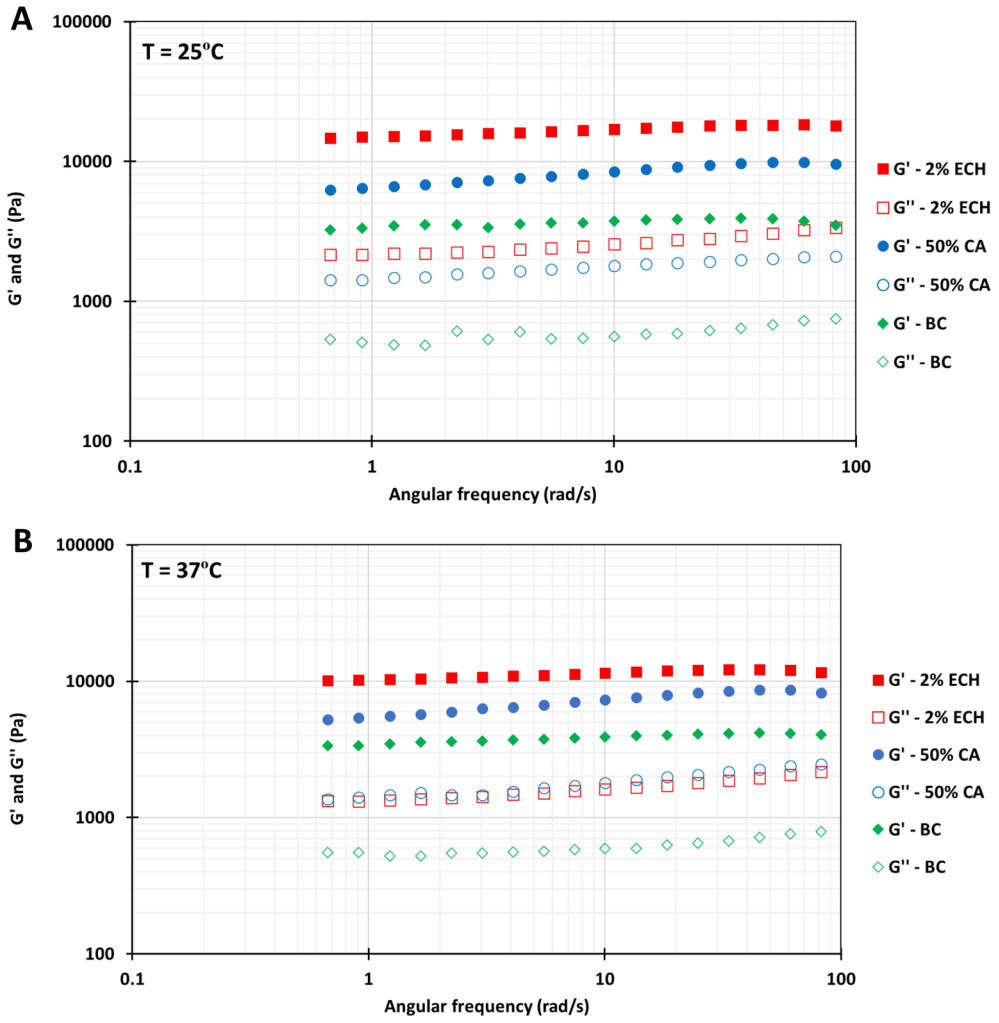

Fig. 6. Viscoelastic properties: storage G' (full symbols) and loss G'' (empty symbols) moduli in function of angular frequency for hydrated BC membranes: unmodified BC; with Citric Acid crosslinking (50 % CA) and with Epichlorohydrin crosslinking (2 % ECH); represented data are an average of three measurements performed over the same membrane and error bars are within each symbol; measurements performed at temperatures 25 °C (**A**) and 37 °C (**B**).

Fig. 6, where the storage G' and loss G'' moduli are represented in function of angular frequency (ω) for unmodified BC, with Citric Acid crosslinking (50 % CA) and with Epichlorohydrin crosslinking (2 % ECH) membranes, at 25 °C and 37 °C. For all the BC membranes we found higher values for G' than G'', in the probed ω range. Being the crosslinked BC membrane with 2 % ECH the one that shows higher values of G' and G''. Moreover, G' and G'' present an almost independent behaviour with respect to ω.

For easy of comparison, in Table 4 are presented the values of G' and G'', and tan δ = G''/G', obtained at ω = 10 rad.s^{-1}, during the measurements performed at temperatures of 25 °C and 37 °C, for the different hydrated BC membranes. Also, in Fig. 7, G' is plotted against temperature for the three tested BC membranes.

Table 4
Mechanical properties of the hydrated BC membranes.

	Temperature (°C)	G' (kPa)	G'' (kPa)	tan δ = G''/G'
Unmodified BC	25	3.74 ± 0.05	0.563 ± 0.002	0.151
2 % ECH		17.06 ± 0.02	2.562 ± 0.002	0.150
50 % CA		8.49 ± 0.04	1.79 ± 0.02	0.211
Unmodified BC	37	3.91 ± 0.09	0.593 ± 0.02	0.152
2 % ECH		11.52 ± 0.01	1.610 ± 0.001	0.140
50 % CA		7.3 ± 0.2	1.79 ± 0.09	0.246

It is known that the higher the G' value, the more pronounced are the elastic properties, and the higher the G'', the more pronounced are the viscous properties. In this sense the storage modulus, G', is a measure of the energy stored and reflects the solid-like component or elastic behaviour of the material. On the other hand, the loss tangent, tan δ = G''/G', is a measure of the damping character of the material. The results obtained for all the hydrated BC membranes, showed that G' > G'', which indicates a prevalence of the elastic component, revealing a pronounced solid-like behaviour, which is also showed by the values of tan δ, always lower than 0.25. Moreover, the slight dependence of G' and G'' on ω may reflect a stable structure with a gel-like character, as expected. These results are comparable with the viscoelastic properties described in the literature for unmodified BC membranes [31]. The hydrated BC membranes produced with 2 % ECH crosslinking showed higher viscoelastic properties than the ones produced with 50 % CA crosslinking. This behaviour is consistent with the higher mechanical performance observed in the dehydrated 2 % ECH membranes during the tensile strength characterization.

Moreover, the crosslinked membranes, 50 % CA and 2 % ECH, presented higher sensitivity to temperature, showing lower values of elastic and viscous moduli at the highest temperature (see Fig. 6 and Table 4),

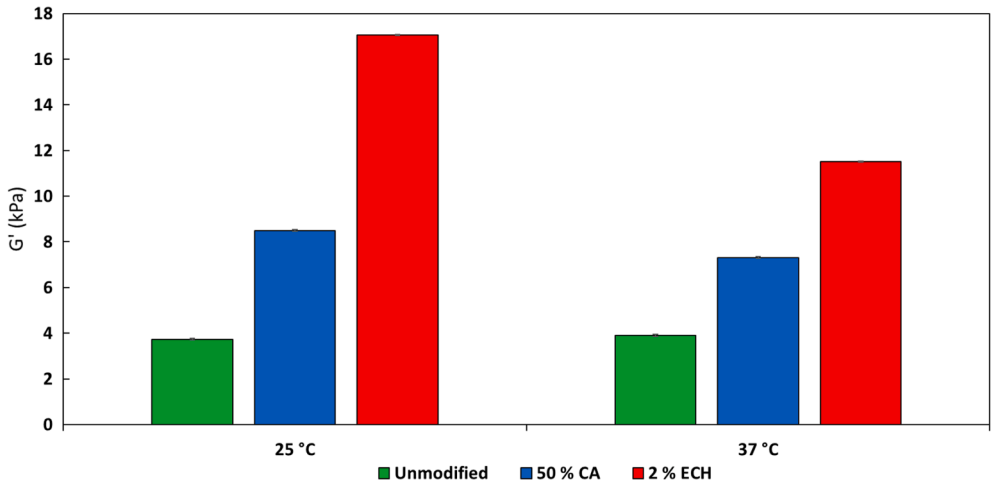

Fig. 7. Storage modulus, G' values obtained at $\omega = 10$ rad.s^{-1}, during measurements performed at 25 °C and 37 °C, for three BC hydrated membranes: unmodified BC; crosslinked with 50% CA and crosslinked with 2% ECH.

while BC membranes showed almost unchanged viscoelastic behaviours for G' and G'', for both temperatures tested. In fact, G' and G'' show an unexpected slight increase with temperature in the case of unmodified BC membranes. Nevertheless, the solid-like character is maintained by the unmodified BC and for the crosslinked 2 % ECH BC membranes, which continue to present low values of tan δ at 37 °C, 0.152 and 0.140 respectively. However, the BC membrane crosslinked with 50 % CA increase the tan δ value with temperature, showing 0.246 at 37 °C, which may reveal a loss in the solid-like character by this membrane.

3.7. Contact angle measurements

The effectiveness of the crosslinking on the wettability of BC membranes was investigated by measuring the static water contact angle (θ) [36]. The wettability of a solid surface is assessed by the contact angle determined according to *Young*'s equation:

$$\gamma_{LV}\cos(\theta) = \gamma_{SV} + \gamma_{SL}$$

Where γ_{LV}, γ_{SV} and γ_{SL} are the interfacial tension between the liquid and vapor, solid and vapor, and solid and liquid, respectively [37].

The incorporation of different surface chemical functionalities may affect surface wettability, charge, roughness, and porosity [38,39]. The static water contact angle values for BC at 0 s, 20 s and 120 s were 76.9 ° ± 4 °, 75.7 ° ± 4 ° and 72.1 ° ± 4 °, respectively. BC crosslinked with 2 % ECH and BC crosslinked with 50 % CA, presented a decrease in the static water contact angle when compared with the unmodified BC (Fig. 8 A). The static water contact angles of BC crosslinked with 2 % ECH at 0 s, 20 s and 120 s, were 65.1 ° ± 3 °, 56.3 ° ± 3 ° and 50.5 ° ± 3 °, respectively and of BC crosslinked with 50 % CA at 0 s, 20 s and 120 s, were 44.1 ° ± 2 °, 40.5 ° ± 2 ° and 40.6 ° ± 2 °. As observed in Fig. 8 A, all the contact angles obtained for the 3 samples were lower than 90 °, which is characteristic of hydrophilic surfaces [40]. It is evident that membranes produced using both methods of crosslinking described in this paper, when compared to the unmodified BC, present an improvement in the wettability capacity (Fig. 8 B). The differences observed after crosslinking can be explained by modifications in surface chemistry, such as intermolecular interactions, (hydrogen and van der Waals bonds), static electricity or hydrophobicity induced by the crosslinking processes [41].

3.8. SEM analysis

Observations were performed both for the membrane surfaces and their cross-sections. Since the membranes were dehydrated during the SEM observations, the pore structure that expands during the hydration and that is responsible for the large water uptake was not visible on any of the observed sample's cross-section, so the images are not presented. The evaluation of the surface morphologies of the membranes shown in Fig. 9, did not show observable differences induced on these surfaces by the crosslinking processes, when compared with the unmodified BC sample. The images reveal a typical nonwoven nanofibrous morphology that is liquid and gas permeable and hydrophilic, all due to the fibre composed membrane morphology, presented in Fig. 9.

4. Conclusions

The hydrophilic character and the BC membrane's high swelling ratio allow, if used in a hydrated state, the maintenance of a moist environment at the wound site, sometimes necessary to enhance recovery and healing. The water retention capacity of the BC membranes prior to the first dehydration is around 99 wt%. The hydrophilic character of the BC membranes, in particular if crosslinked, enables the reversible swelling and de-swelling of the membrane, when used in the dehydrated state, which allows its application on heavily exudating wounds. The water retention capacity of the BC membranes after the first dehydration was found to be around 77 wt% for the membranes crosslinked with 2 % ECH and around 82 wt% for the membranes crosslinked with 50 % CA. Since these membranes are the ones, for each crosslinking method, that present the lowest reduction in the water retention capacity, when compared with the unmodified BC, they were studied in more detail. By crosslinking the BC membranes, the decrease in the water retention capacity after the first dehydration was reduced with respect to the same of unmodified BC membranes. The efficiency of the crosslinking was evident in the maintenance of a higher water retention capacity, a higher water uptake rate and also for the good mechanical properties, in the last case for both in the hydrated and dehydrated states. Both hydrated and dehydrated and both unmodified and crosslinked membranes present mechanical properties compatible with those of the human skin and are robust enough to be used in the proposed applications.

The two crosslinking methods, with CA and with ECH, resulted in differences in terms of mechanical properties and water uptake capacity. The CA crosslinking showed advantages in the water uptake capacity and in the fact that CA is an innocuous compound, entitling it as better suited for biomedical applications.

This works demonstrates that these BC membranes present physical properties suitable for biomedical applications.

Data availability statement

No datasets have been used.

Compliance with Ethical Standards

Funding: This study was funded by by National funds from FCT -

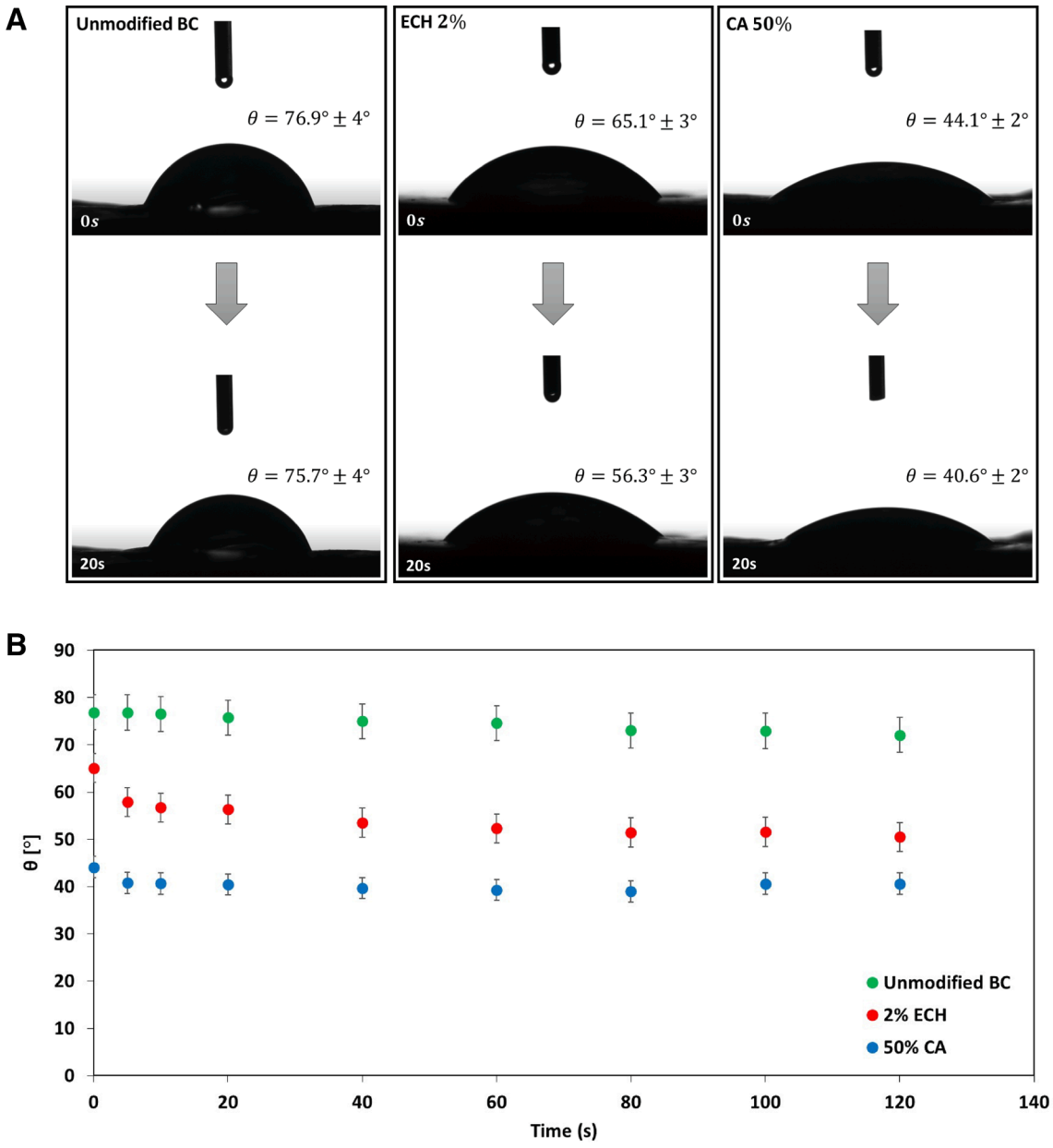

Fig. 8. Wettability measurements: (**A**) Photos acquired immediately after droplet deposition (0 s) and after 20 s using the *OCA20* software for the water contact angle of the unmodified BC, 2 % ECH and 50 % CA membranes. (**B**) Plot of water contact angle for unmodified BC, 2% ECH and 50 % CA membranes versus time. The contact angle values presented are an average of six independent measurements with standard deviation below 4°.

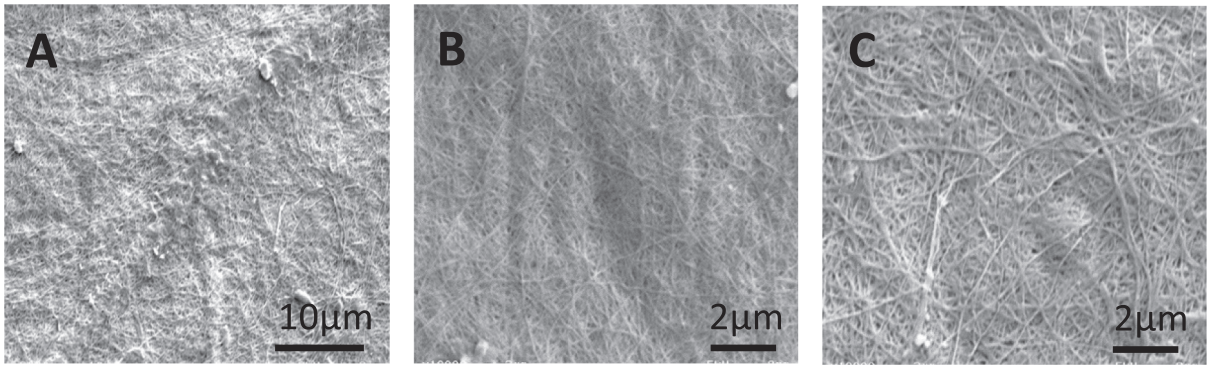

Fig. 9. SEM pictures of the membranes surface. (**A**) unmodified BC; (**B**) BC crosslinked with 50 % CA and (**C**) BC crosslinked with 2 % ECH.

Fundação para a Ciência e a Tecnologia, I.P., in the scope of the project UIDP/04378/2020 and UIDB/04378/2020 of the Research Unit on Applied Molecular Biosciences - UCIBIO and the project LA/P/0140/2020 of the Associate Laboratory Institute for Health and Bioeconomy – i4HB as well as project reference UID/CTM/50025/2020 of the Research Unit CENIMAT – I3N. This work was also supported by FCT through grant PTDC/BIA-MIC/31645/2017 (awarded to R.G.S.).

Ethical approval

This article does not contain any studies with human participants or animals performed by any of the authors.

CRediT authorship contribution statement

Ana P.C. Almeida: Data curation, Formal analysis, Writing – review & editing. **João N. Saraiva:** Data curation, Formal analysis, Writing – review & editing. **Gonçalo Cavaco:** Data curation, Formal analysis, Writing – review & editing. **Raquel P. Portela:** Data curation, Formal analysis, Writing – review & editing. **Catarina R. Leal:** Data curation, Formal analysis, Writing – review & editing. **Rita G. Sobral:** Conceptualization, Funding acquisition, Resources, Writing – review & editing. **Pedro L. Almeida:** Conceptualization, Writing – original draft, Writing – review & editing.

Declaration of Competing Interest

The authors declare the following financial interests/personal relationships which may be considered as potential competing interests: Rita G. Sobral reports financial support was provided by Foundation for Science and Technology. Pedro L. Almeida reports financial support was provided by Foundation for Science and Technology.

References

[1] S.N. Fernandes, P.L. Almeida, N. Monge, L.E. Aguirre, D. Reis, C.L.P. de Oliveira, A. M.F. Neto, P. Pieranski, M.H. Godinho, Mind the Microgap in Iridescent Cellulose Nanocrystal Films, Adv. Mater. 29 (2) (2017) 1603560.
[2] J.L.W. Morgan, J.T. McNamara, M. Fischer, J. Rich, H.-M. Chen, S.G. Withers, J. Zimmer, Observing cellulose biosynthesis and membrane translocation in crystallo, Nature 531 (7594) (2016) 329–334.
[3] M. Martínez-Sanz, D. Mikkelsen, B. Flanagan, M.J. Gidley, E.P. Gilbert, Multi-scale model for the hierarchical architecture of native cellulose hydrogels, Carbohydr. Polym. 147 (2016) 542–555.
[4] R. Portela, C.R. Leal, P.L. Almeida, R.G. Sobral, Bacterial cellulose: a versatile biopolymer for wound dressing applications, Microb. Biotechnol. 12 (4) (2019) 586–610.
[5] P. Jacek, et al., Optimization and characterization of bacterial nanocellulose produced by Komagataeibacter rhaeticus K3, Carbohydr. Polym. Technol. Appl. 2 (2021) 100022.
[6] W. Czaja, A. Krystynowicz, S. Bielecki, R. Brownjr, Microbial cellulose–the natural power to heal wounds, Biomaterials 27 (2) (2006) 145–151.
[7] N. Pogorelova, et al., Bacterial Cellulose Nanocomposites: Morphology and Mechanical Properties, 13(12) (2020) 2849.
[8] B. Mbituyimana, et al., Bacterial cellulose-based composites for biomedical and cosmetic applications: Research progress and existing products, Carbohydr. Polym. 273 (2021) 118565.
[9] M. Fursatz, et al., Functionalization of bacterial cellulose wound dressings with the antimicrobial peptide epsilon-poly-L-Lysine, Biomed. Mater. 13 (2) (2018) 025014.
[10] J.S. Capes, H.Y. Ando, R.E. Cameron, Fabrication of polymeric scaffolds with a controlled distribution of pores, J. Mater. Sci. - Mater. Med. 16 (12) (2005) 1069–1075.
[11] S.T. Schrecker, P.A. Gostomski, Determining the water holding capacity of microbial cellulose, Biotechnol. Lett. 27 (19) (2005) 1435–1438.
[12] S.A. Geravand, R. Khajavi, M.K. Rahimi, M.S. Ghiyasvand, A. Meftahi, Improving some structural and biological characteristics of bacterial cellulose by cross-linking, J. Appl. Polym. Sci. 139 (18) (2022) 52056.
[13] S.-T. Chang, L.-C. Chen, S.-B. Lin, H.-H. Chen, Nano-biomaterials application: Morphology and physical properties of bacterial cellulose/gelatin composites via crosslinking, Food Hydrocoll. 27 (1) (2012) 137–144.
[14] A. Meftahi, R. Khajavi, A. Rashidi, M.K. Rahimi, A. Bahador, Preventing the collapse of 3D bacterial cellulose network via citric acid, J. Nanostruct. Chem. 8 (3) (2018) 311–320.
[15] H. Qi, Y. Huang, B. Ji, G. Sun, F.-L. Qing, C. Hu, K. Yan, Anti-crease finishing of cotton fabrics based on crosslinking of cellulose with acryloyl malic acid, Carbohydr. Polym. 135 (2016) 86–93.
[16] A.N. Frone, et al., Bacterial cellulose sponges obtained with green cross-linkers for tissue engineering, Mater. Sci. Eng. C Mater. Biol. Appl. 110 (2020) 110740.
[17] R.R. Schio, J.O. Gonçalves, E.S. Mallmann, D. Pinto, G.L. Dotto, Development of a biosponge based on Luffa cylindrica and crosslinked chitosan for Allura red AC adsorption, Int. J. Biol. Macromol. 192 (2021) 1117–1122.
[18] Q.Z. Yang, C.J. Fan, X.G. Yang, L.Q. Liao, L.J. Liu, Facile synthesis of biocompatible polyglycerol hydrogel based on epichlorohydrin, J. Appl. Polym. Sci. 133 (21) (2016) n/a–n/a.
[19] D.T.B. De Salvi, H. da S. Barud, O. Treu-Filho, A. Pawlicka, R.I. Mattos, E. Raphael, S.J.L. Ribeiro, Preparation, thermal characterization, and DFT study of the bacterial cellulose, J. Therm. Anal. Calorim. 118 (1) (2014) 205–215.
[20] K. Potivara, M. Phisalaphong, Development and Characterization of Bacterial Cellulose Reinforced with Natural Rubber, Materials (Basel, Switzerland) 12 (14) (2019) 2323.
[21] W.-C. Lin, C.-C. Lien, H.-J. Yeh, C.-M. Yu, S.-H. Hsu, Bacterial cellulose and bacterial cellulose–chitosan membranes for wound dressing applications, Carbohydr. Polym. 94 (1) (2013) 603–611.
[22] I.M. Bodea, et al., Optimization of Moist and Oven-Dried Bacterial Cellulose Production for Functional Properties, **13**(13) (2021) 2088.
[23] M. Ul-Islam, T. Khan, J.K. Park, Water holding and release properties of bacterial cellulose obtained by in situ and ex situ modification, Carbohydr. Polym. 88 (2) (2012) 596–603.
[24] J. Diaz-Ramirez, L. Urbina, A. Eceiza, A. Retegi, N. Gabilondo, Superabsorbent bacterial cellulose spheres biosynthesized from winery by-products as natural carriers for fertilizers, Int. J. Biol. Macromol. 191 (2021) 1212–1220.
[25] P. Kalyani, M. Khandelwal, Modulation of morphology, water uptake/retention, and rheological properties by in-situ modification of bacterial cellulose with the addition of biopolymers, Cellulose 28 (17) (2021) 11025–11036.
[26] E. Madivoli, P. Kareru, A. Gachanja, S. Mugo, M. Murigi, P. Kairigo, C. Kipyegon, J. Mutembei, F. Njonge, Adsorption of Selected Heavy Metals on Modified Nano Cellulose, J. Int. Res. J. Pure Appl. Chem. 12 (3) (2016) 1–9.
[27] R. Brandes, et al., Preparation and characterization of bacterial cellulose/Tio2 hydrogel nanocomposite, J. Nano Res. 43 (2016) 73–80.
[28] I.A. Udoetok, L.D. Wilson, J.V. Headley, "Pillaring Effects" in Cross-Linked Cellulose Biopolymers: A Study of Structure and Properties, Int. J. Polym. Sci. 2018 (2018) 1–13.
[29] S.-Q. Chen, D. Mikkelsen, P. Lopez-Sanchez, D. Wang, M. Martinez-Sanz, E. P. Gilbert, B.M. Flanagan, M.J. Gidley, Characterisation of bacterial cellulose from diverse Komagataeibacter strains and their application to construct plant cell wall analogues, Cellulose 24 (3) (2017) 1211–1226.
[30] S. Wang, F. Jiang, X.u. Xu, Y. Kuang, K. Fu, E. Hitz, L. Hu, Super-Stiff Macrofibers with Aligned, Long Bacterial Cellulose Nanofibers, Adv. Mater. 29 (35) (2017) 1702498.
[31] S.Q. Chen, et al., The influence of alkaline treatment on the mechanical and structural properties of bacterial cellulose, Carbohydr. Polym. 271 (2021).
[32] J. Huang, D. Li, M. Zhao, P. Lv, L. Lucia, Q. Wei, Highly stretchable and bio-based sensors for sensitive strain detection of angular displacements, Cellulose 26 (5) (2019) 3401–3413.
[33] J.F. Menegasso, N.A.C. Moraes, T.P. Vásquez, F.A. Felipetti, R.V. Antonio, R. C. Dutra, Modified montmorillonite-bacterial cellulose composites as a novel dressing system for pressure injury, Int. J. Biol. Macromol. 194 (2022) 402–411.
[34] A.N. Nakagaito, S. Iwamoto, H. Yano, Bacterial cellulose: the ultimate nano-scalar cellulose morphology for the production of high-strength composites, Appl. Phys. a-Mater. Sci. Process. 80 (1) (2005) 93–97.
[35] M. Pawlaczyk, M. Lelonkiewicz, M. Wieczorowski, Age-dependent biomechanical properties of the skin, Postepy dermatologii i alergologii 30 (5) (2013) 302–306.
[36] T. Huhtamäki, X. Tian, J.T. Korhonen, R.H.A. Ras, Surface-wetting characterization using contact-angle measurements, Nat. Protoc. 13 (7) (2018) 1521–1538.
[37] S.-J. Park, M.-K. Seo, Chapter 3 - Solid-Liquid Interface, in Interface Science and Technology, S.-J. Park and M.-K. Seo, Editors, Elsevier, 2011, p. 147–252.
[38] S. Gonçalves, J. Padrão, I.P. Rodrigues, J.P. Silva, V. Sencadas, S. Lanceros-Mendez, H. Girão, F. Dourado, L.R. Rodrigues, Bacterial Cellulose As a Support for the Growth of Retinal Pigment Epithelium, Biomacromolecules 16 (4) (2015) 1341–1351.
[39] S. Leal, C. Cristelo, S. Silvestre, E. Fortunato, A. Sousa, A. Alves, D.M. Correia, S. Lanceros-Mendez, M. Gama, Hydrophobic modification of bacterial cellulose using oxygen plasma treatment and chemical vapor deposition, Cellulose 27 (18) (2020) 10733–10746.
[40] S. Rbihi, et al., Contact Angle Measurements of Cellulose based Thin Film composites: wettability, surface free energy and surface hardness, Surf. Interfaces 21 (2020).
[41] N. Boonchai, et al., Chemical Functionalization of Bacterial Cellulose Film for Enhancing Output Performance of Bio-Triboelectric Nanogenerator, Biointerf. Res. Appl. Chem. 12 (2) (2021) 1587–1600.